Fuel 99 (2012) 188–196

Contents lists available at SciVerse ScienceDirect

Fuel

journal homepage: www.elsevier.com/locate/fuel

Mercury chemistry on brominated activated carbon

Erdem Sasmaz [a,*], Abby Kirchofer [a], Adam D. Jew [b], Arindom Saha [c], David Abram [c], Thomas F. Jaramillo [c], Jennifer Wilcox [a]

[a] Department of Energy Resources Engineering, Stanford University, Stanford, CA 94305, United States
[b] Department of Geological and Environmental Sciences, Stanford University, Stanford, CA 94305, United States
[c] Department of Chemical Engineering, Stanford University, Stanford, CA 94305, United States

HIGHLIGHTS

- Hg is adsorbed on brominated AC as Hg^{2+} at both 30 °C and 140 °C.
- Chemisorption is the likely adsorption mechanism of Hg.
- Hg interacts with two Br atoms at a distance of 2.55 ± 0.01 Å inside the C matrix.
- Hg s- and Hg p-states hybridize with Br and C p-states to form stable complexes.

ARTICLE INFO

Article history:
Received 20 October 2011
Received in revised form 26 March 2012
Accepted 20 April 2012
Available online 7 May 2012

Keywords:
Mercury
Activated carbon
Bromine
XPS
EXAFS

ABSTRACT

Activated carbon-based sorbents are the most widely tested sorbents for mercury removal in coal-fired power plants. A major problem in mercury removal is the limited understanding of the mechanism associated with elemental mercury (Hg^0) oxidation and its subsequent adsorption. This work investigates the possible binding mechanism of Hg^0 onto brominated fiber and powder activated carbon sorbents through packed-bed experiments in a stream of air. To better understand the mechanisms involved, a combination of spectroscopy and quantum mechanical modeling were used to characterize the sorption process. X-ray photoelectron spectroscopy (XPS) and extended X-ray absorption fine structure (EXAFS) spectroscopy were used to analyze the surface and bulk chemical compositions of brominated activated carbon sorbents reacted with Hg^0. It was found that Hg^0 is oxidized at the brominated carbon surfaces at both 30 °C and 140 °C. The oxidation state of adsorbed Hg is found to be Hg^{2+}, and coordinated to two Br atoms with no detectable bonding between Hg and O. Though plane-wave density functional theory (DFT) and density of states (DOSs) calculations indicate that Hg is more stable when it is bound to the edge C atom interacting with a single Br bound atop of Hg, a model that includes an interaction between the Hg and an additional Br atom matches best with experimental data obtained from EXAFS spectroscopy. Because the most stable structures optimized in the DFT simulations were not found on the samples analyzed using EXAFS spectroscopy, Hg surface reactions on the carbon surface are thought to be kinetically controlled.

1. Introduction

The US is putting significant effort into decreasing harmful emissions into the environment through regulations such as the EPA's Clean Air Interstate Rule (CAIR) and the Clean Air Mercury Rule (CAMR), which place caps on NO_x, SO_x, and Hg emissions [1]. Recently, on March 2011 the EPA stated that all hazardous air pollutants must have emission standards and proposed that for existing sources in the category, that the standards are at least as stringent as the emission reductions achieved by the average of the top 12% best controlled sources for source categories with 30 or more sources. With this new rule, a reduction of mercury from coal emissions of approximately 90% is anticipated [1]. Recent studies indicate that mercury content in coal varies between 0.01 and 1.5 g per ton of coal, with world coal consumption in 2006 estimated at 6118 million tons per year [2]. In 1999, the EPA estimated that US coal combustion emits approximately 50 tons Hg/year into the air [1], while global emissions are approximately 810 tons Hg/year [2]. The need for effective sorbent materials to capture harmful pollutants of flue gases continues to increase as coal consumption increases worldwide.

Typically, activated carbon injection is used to capture oxidized mercury [3]. A major limitation with using activated carbon is that in flue gases with low halogen concentrations a large amount of activated carbon needs to be added to the system to effectively

* Corresponding author.
E-mail address: sasmaz@cec.sc.edu (E. Sasmaz).

0016-2361/$ - see front matter © 2012 Elsevier Ltd. All rights reserved.
http://dx.doi.org/10.1016/j.fuel.2012.04.036

control Hg^0. Depending on the system conditions, an activated carbon-to-mercury mass ratio of at least 3000–20,000 (C/Hg) can be necessary to achieve 90% Hg removal [4]. Huggins et al. [5] tested various activated carbon (AC) sorbents in a simulated flue gas containing gaseous Hg^0 and characterized them using X-ray absorption fine structure (XAFS) spectroscopy. They observed that Hg sorption is dominated by anionic species, such as sulfides, chlorides, oxides and iodides present within the matrix of the sorbent or bound to the sorbent surface. The results of the XAFS spectra obtained from mercury adsorbed on these tested AC samples indicate that little or no Hg^0 was present and that Hg-anion chemical bonds are formed on the sorbent materials, suggesting chemisorption to be the primary adsorption mechanism. From these results, they infer that an oxidation process is involved in the ultimate capture of Hg^0 by bonding to iodine (I), chlorine (Cl), sulfur (S) or oxygen (O) anionic species on the carbon surface. Hutson et al. [6] characterized chlorinated AC and brominated AC using X-ray absorption spectroscopy (XAS) and X-ray photoelectron spectroscopy (XPS) after exposing the carbons to Hg^0-laden flue gas. Due to the low coverage of Hg on the carbon, they could not determine the speciation of Hg. Since homogenous oxidation was not observed in their experiments, they proposed that Hg capture by chlorinated and brominated carbons takes place by surface oxidation of Hg^0 with subsequent adsorption on the surface [6]. They concluded that Hg was expected to bind on the chlorinated and brominated sites of carbon and even in some cases mercury-sulfate species were expected to form due to the presence of sulfur dioxide (SO_2) in the flue gas. Olson et al. [7] suggested that acidic sites on the surface are responsible for Hg^0 capture on AC. They propose that Hg^0 has the propensity to be oxidized by donating its electrons to a surface or another gas-phase molecule; therefore, in its elemental state, Hg^0 acts as a Lewis base with the desire to interact with an acidic site forming a strong C–Hg covalent bond on the carbon surface. However, in their work they were not able to determine the oxidation states of the various surface-bound Hg due to the interference with silicon (Si), which was inherently present in the form of ash in their coal-derived AC sorbents [8].

The speciation of Hg adsorbed on carbon surfaces has yet to be elucidated, and the adsorption mechanism and the effects of flue gas components on Hg adsorption are not well understood. This current work represents a first step in determining the surface chemistry of Hg interacting with powdered AC in the presence of air at 140 °C through surface and bulk characterization using XPS and EXAFS. Additional Hg adsorption experiments have been performed at 30 °C to determine the surface-bound Hg species on powdered AC using XPS. The plane-wave density functional theory calculations (DFT) are carried out to identify the interaction of Hg with Br bound graphene edge sites. This work has been carried out in an attempt to simplify the chemistry of Hg^0 on AC surfaces and thereby provide a foundation for understanding more complex systems.

2. Methodologies

2.1. Sorbent preparation

Mercury-adsorbed to brominated AC samples were prepared to identify the Hg oxidation state, bond distance, binding ligands, and number of ligands (coordination) using both XPS and EXAFS spectroscopy. To understand Hg adsorption in an air environment, a packed-bed reactor system was constructed (Fig. 1) to prepare samples for spectroscopic analysis. Sorbent particles were placed in the 1.27 cm-diameter quartz packed-bed reactor. The reactor was covered with a 50 cm-long ceramic fiber heater to conduct tests at controlled temperatures while also providing a uniform

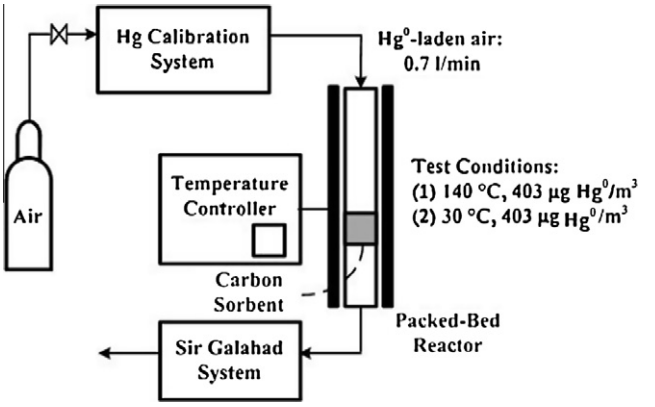

Fig. 1. Schematic of the packed-bed reactor system.

temperature profile in the reactor. Elemental Hg vapor was introduced into the system using a Hg calibration system (PSA 10.536 Mercury Calibration System, PS Analytical). The concentration of Hg^0 in the outlet flow was measured using a PSA 10.525 Sir Galahad Hg analyzer (PS Analytical). The results described here are based upon pure Hg^0 injection with air over commercially-available brominated AC powder (AC–Br) (DARCO Hg–LH, Norit Americas Inc.), and brominated activated carbon fiber (ACF–Br) (Illinois State Geological Survey and University of Illinois) sorbents. The typical surface area of powder and fiber activated carbon sorbents can vary between 100–800 m^2/g [9]. A variety of conditions were considered, i.e. (1) 140 °C, 403 μg/m^3 Hg^0, and (2) 30 °C, 403 μg/m^3 Hg^0, all in air with a flow rate of 0.7 L/min. Typical flue gas conditions in a commercial-scale AC injection process contain 15 μg/m^3 Hg, which is below the concentrations used in the experiments. High Hg concentrations were used to decrease testing time and increase signal intensity of the Hg4f spectrum in XPS analysis. The powdered AC sorbents, prepared from lignite-based coal, contain Si by nature, which interferes with the spectra of oxidized Hg compounds due to the similarity in binding energies of Hg4f and Si2p electrons [10]. Mercury adsorption tests were also conducted at a lower temperature, i.e. 30 °C, to promote Hg-surface interactions to enhance the intensity of the Hg spectrum in the presence of Si. All the tests were conducted until the outlet Hg concentration approached the inlet Hg concentration to maximize the amount of Hg adsorbed on the carbon surface. The goal of this work is to investigate the chemistry of Hg on AC sorbents; therefore, breakthrough curves of each sorbent were not generated.

2.2. XPS analysis

The XPS analyses were performed using a Physical Electronics (PHI) 5000VersaProbe Scanning XPS system at the Stanford Nanocharacterization Laboratory at Stanford University (Stanford, CA). Spectra were collected using monochromatic Al Kα radiation at 1486 eV. XPS is a surface-sensitive technique and the photoelectrons coming only from the top ~5 nm of the surface can be detected. The data reduction was carried out using the PHI MultiPak Software package [11]. All the spectra were calibrated to the C1s peak located at 284.6 eV. Due to the high vacuum of the analysis chamber (i.e. 10^{-10} Torr) it is anticipated that loosely-bound physisorbed Hg will likely be removed leading to the assumption that the surface-bound Hg observed must be chemisorbed.

2.3. EXAFS analysis

Mercury L_{III}-edge EXAFS spectra were collected at wiggler beamline 7–3 at Stanford Synchrotron Radiation Lightsource

(SSRL) using a LN_2 cooled Si(220) double-crystal monochromator in the phi = 90° orientation. Higher harmonics in the X-ray beam were removed using a harmonics mirror. Data was collected at 3.0 GeV with a current of 100 mA. Hg L_{III}-edge EXAFS spectra were collected in fluorescence mode using a 30-element germanium array detector along with three sets of ion chambers. A $HgCl_2$ reference compound was placed between the I_1 and I_2 ion chambers to serve as a continuous energy calibration standard. AC samples were loaded into an aluminum sample holder and sealed with Kapton® tape. EXAFS spectra were collected at 80 K and ambient pressure using a LHe cryostat. To determine if elemental Hg was present within the samples, a modified version of the slow-cooling Hg L_{III}-edge EXAFS method developed by Jew et al. was used [12]. Samples were loaded into the sample holders and sealed glass container prior to being cooled in a −20°C freezer for 30 min. The sample was then immediately transferred to a −80 °C freezer for an additional 30 min to allow any elemental Hg to slowly crystallize into α-Hg(0), which, if present in the sample, would result in an identifiable EXAFS pattern [12]. The sample holder was taken from the −80 °C freezer and placed directly into LN_2 where it was mounted onto the LHe cryostat sample rod. Up to 16 scans collected to a k of 15 $Å^{-1}$ were taken to improve the signal-to-noise ratio. Background subtraction and analysis of the EXAFS spectra was performed using theoretical pathways created by FEFF 6L and the SixPACK XAS analysis software package [13–15]. Shell-by-shell fitting of the mercury L_{III} k^3-weighted EXAFS spectra was done over a k range of 3–15 $Å^{-1}$ with goodness of fit being determined by a reduced χ^2.

2.4. Computational details

Electronic structure calculations based on plane-wave density functional theory (DFT) were carried out in parallel with experimental work in order to determine the surface reactivity and subsequent thermodynamic stability of surface-bound Hg species on simulated AC surfaces as well as to investigate the effects of Br surface functional groups. DFT calculations were carried out using the Vienna ab initio Simulation Package (VASP) [16]. The projector augmented wave (PAW) method was used to describe the ion–electron interactions [17]. Electron exchange–correlation functionals were represented with the generalized-gradient approximation (GGA), with the Perdew, Burke and Ernzerhof (PBE) model used for the nonlocal corrections [18]. The energy cutoff for the plane-wave expansion was 400 eV and Methfessel, and Paxton Gaussian smearing of order one was used with a width of 0.2 eV to accelerate convergence of the total energy calculations [19]. The surface Brillouin zone integration was calculated using a gamma-centered $5 \times 5 \times 1$ (for slab) or $5 \times 1 \times 1$ (for ribbon) Monkhorst–Pack mesh [20]. Geometric optimization was performed using the conjugate-gradient algorithm until the absolute value of the forces on unconstrained atoms was less than 0.03 eV/Å.

Radovic showed that the reactivity of AC can be studied using a simplified graphene model in which a single graphene sheet mimics the AC surface [21]. Many studies have used graphene zigzag edge sites with unsaturated edge atoms to simulate the active sites on carbonaceous surfaces [22–26]. Using a 9-ring deep graphene ribbon model, electronic structure calculations have been carried out to determine the most stable concentrations and configurations of hydrogen (H), bromine (Br), and Hg atoms on the edge sites. Details of the model are described elsewhere [10]. The partial density of states (DOSs) were calculated by projecting the electronic wave functions onto spherical harmonics centered on Hg, carbon (C), and Br atoms to determine the potential mechanisms associated with Hg binding to edge sites of graphene. The integral of the DOS up to the Fermi level is proportional to the number of electrons participating in bonding and local reactivity. In general, the DOS analysis allows for an understanding of how electrons are covalently shared between different atoms. The strong binding is expected if the bonding states are shifted down below the Fermi level indicating occupancy.

3. Results and discussion

Preliminary tests were conducted to assess the performance of the packed-bed reactor system as well as to determine the experimental conditions necessary for preparing sorbent samples for characterization to determine Hg^0 oxidation and binding mechanisms. The most efficient configuration for Hg capture involved mixing the carbon sorbent with sand (e.g. 30 mg AC/6 g sand) and supporting this mixture with quartz wool. However, both sand and quartz wool contain Si, an element whose main XPS lines coincide with those of oxidized Hg. Dilution is an additional complication, as the mole percent of Hg in the sample decreases significantly after mixing with sand, remaining below the detection limit of XPS. To minimize this problem, all the experiments were carried out in the packed-bed reactor in the absence of sand and quartz wool.

Table 1 shows the compositional analysis of AC–Br and ACF–Br sorbents before exposure to Hg. Since the powder sorbents are derived from lignite coal, their surface composition includes elements such as calcium (Ca), magnesium (Mg), aluminum (Al), and Si. For AC–Br sorbents, S was found to be present on the carbon surface. Compositional analysis of the S2p core-level XPS spectra before exposure to Hg suggests that 85% of the S on the surface exists in an oxidized state, as sulfate (SO_4^{2-}), with binding energies in the region of 169.7 eV. Other studies also found a significant presence of surface-bound sulfate, consistent with this work [27,28]. The surface mole composition of Si is found to be 0.7% for the AC–Br sample before reaction. This concentration is anticipated to be much higher than that of Hg after reaction (<0.1%); therefore, it is expected that the Si2p and Hg4f spectra will interfere with each other between 99.5 eV and 104 eV. The surface composition

Table 1
Elemental compositional analysis of powdered and fiber-based brominated AC before and after exposure to Hg.

Compositional analysis (%)						
	AC–Br	AC–Br 30 °C air + Hg	AC–Br 140 °C air + Hg	ACF–Br	ACF–Br air + Hg	ACF–Br air
C	78.4	77.7	71.7	93	94.9	93.8
O	16	15.5	24	5.3	3.9	4.6
Ca	1.9	1.9	1.4	1	0.7	1
Mg	0.3	0.2	<0.1	–	–	–
Si	0.7	1.9	0.9	–	–	–
S	0.7	0.7	0.3	–	–	–
Na	1.5	1.5	1.3	–	–	–
Br	0.5	0.5	0.3	0.7	0.4	0.5
Hg	–	0.1	<0.1	–	0.1	–

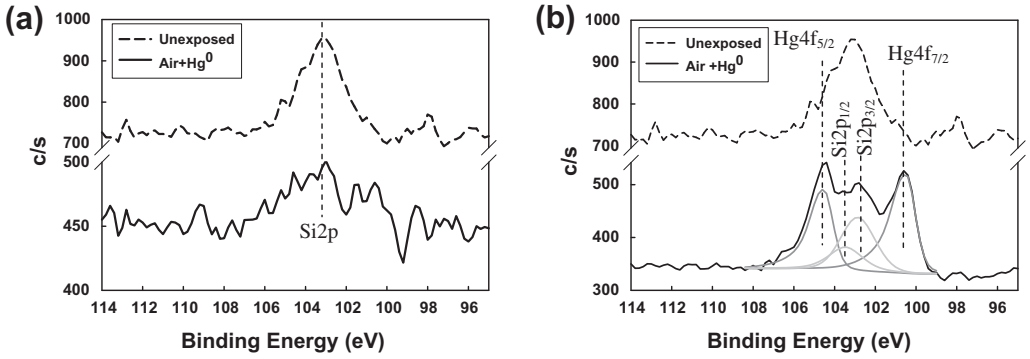

Fig. 2. Hg4f core-level XPS spectra for AC–Br sorbents exposed to 403 μg/m^3 Hg^0 at (a) 140 °C and (b) 30 °C and compared with unexposed AC–Br.

Table 2
XPS binding energies for Hg^0, Hg–Br, HgO and mercuric carbide references and Hg-containing brominated AC.

Refs. [27,28]	$Hg4f_{5/2}$ (eV)	$Hg4f_{7/2}$ (eV)	ΔE (eV)
Hg^0	104	99.9	4.1
$HgBr_2$		101	
Hg_2Br_2		100.7	
HgO	104.8	100.8	4.0
Mercuric carbide		100.8–101.3	
[a]Hutson et al. [6]			
AC–Br	104.7	100.8	3.9
Current work			
AC–Br 403 μg/m^{3}140 °C	105.0	100.9	4.1
ACF–Br 403 μg/m^{3}140 °C	104.6	100.6	4.0
AC–Br 403 μg/m^{3}30 °C	104.7	100.7	4.0

[a] In this study all of the spectra are calibrated to the binding energy of C1s photoelectrons at 284.6 eV, whereas Hutson et al. calibrated all their spectra at 285.2 eV. In order to facilitate direct comparison, the Hg4f binding energies shown above for the work reported in Hutson et al. are shifted by 0.6 eV vs. the original reference.

investigation carried out from an XPS survey scan of the ACF–Br sorbent only showed C, O, Ca and Br compounds without the presence of Si and other metals. The Hg4f core-level XPS spectra for Hg-containing AC–Br sorbents are shown in Fig. 2 at 140 °C and 30 °C. It is challenging to uniquely assign XPS spectral features to specific Hg compounds using XPS since the $Hg4f_{7/2}$ binding energies for numerous compounds containing oxidized Hg lie in the tight range from 100.7 eV (Hg_2Br_2) to 101.4 eV ($HgCl_2$). Also, the Si2p spectral lines of Si–C, silicon dioxide (SiO_2) and Si compounds are expected to be in the region between 98.5 eV and 104 eV. The Si2p core-level spectra can be separated from Hg4f spectra by using the area of the Si2s core-level spectra and the intensity ratios of the two Si spectral lines [10]. Table 2 provides a summary of the XPS of Hg and Br binding energies for Hg–Br reference compounds [29,30] and for the Hg-containing brominated AC sorbent investigated in the current work compared against the study carried out by Hutson et al. [6]. In the case of AC–Br tested at 403 μg/m^3 and 140 °C, $Hg4f_{7/2}$ and $Hg4f_{5/2}$ spectral lines are found to be in the binding region of 100.9 and 105 eV, respectively. Although this Hg doublet clearly indicates that the Hg on the surface is oxidized, it does not uniquely identify the Hg species.

It is known that Hg adsorption on AC is an exothermic process [31] and that lower temperatures increase Hg adsorption on the surface; therefore, the sorbent experiments carried out at 30 °C were expected to have high enough surface Hg concentrations for XPS detection. In fact, the Hg4f doublet is clearly observed in Fig. 2b, with the $Hg4f_{7/2}$ and $Hg4f_{5/2}$ lines centered at 100.7 eV and 104.7 eV, respectively, indicating that the Hg is in an oxidized state. As shown in Fig. 2b, the intensity of Hg4f doublet is slightly enhanced and the two distinguishing oxidized $Hg4f_{7/2}$ and $Hg4f_{5/2}$ peaks are centered around 100.7 and 104.7 eV, respectively. Reference data in Table 2 reveals binding energy positions for various oxidized forms of Hg: $HgBr_2$, HgO, Hg_2Br_2 or mercuric carbide. The latter three are likely possibilities for the case of Hg sorption onto the AC–Br surface. To help identify which of these species are most likely on the surface, DFT calculations and EXAFS measurements were employed (see below).

An additional Hg adsorption test was carried out on an ACF–Br sorbent at 140 °C, in which Si was hardly observed, allowing for the expected Hg4f core-level spectra to be determined clearly. As shown in Fig. 3a, the Hg4f core-level XPS spectra for the ACF–Br sorbent reveals the Hg doublet at binding energies of 100.6 and 104.6 eV, respectively. These energies are consistent with those determined for AC–Br. Composition analyses of the Hg4f spectral lines indicate that spectral lines are found to shift above the binding energy of 99.7 eV, suggesting that Hg bound on the surface is in the form of oxidized Hg, which is consistent with the results of Hutson et al. [6]. Even at low temperature, i.e. 30 °C, Hg^0 is not detected, suggesting that the adsorption mechanism of Hg is either oxidative chemisorption at both 30 °C and 140 °C or that weakly bound Hg^0 is removed in the ultra high vacuum environment.

A high-resolution scan of the Br3d region of the untested ACF–Br sorbent shows $Br3d_{5/2}$ and $Br3d_{3/2}$ doublet at 68.1 and 69.1 eV as shown in Fig. 3b, attributed to different carbon-bound Br compounds. This is also consistent with previous studies, where they reported similar Br3d binding energy peaks for Darco Hg–LH and non-halogenated AC and brominated carbon nanotubes [6,32–35]. Papirer et al. [33] studied brominated carbon black compounds with XPS and determined different Br compounds on the carbon surface depending on the bromination method and subsequent heating. The $Br3d_{5/2}$ peak at 67.4 (±0.2) eV was reported to be C_n–Br_2 surface complexes, in which Br was strongly bound and resistant to heating at 450 °C. The physisorbed Br produced a $Br3d_{5/2}$ peak between 67.8 (±0.2) eV and 69.2 (±0.2) eV and is attributed to surface-bound HBr compounds, which are likely desorbed from the surface after vacuum outgassing at 100 °C for 4 days [33]. Bromine sp^2 and sp^3 hybridized covalent bonds to C atoms were also previously suggested to be at 70.0 (±0.2) eV [31]. Based on these assignments, the Br3d spectra in Fig. 3b can be attributed to the formation of all three of these Br-surface complexes on the C. Surface composition analysis of the ACF–Br sorbent reveals that the mole percentage of Br decreases to 0.5% and 0.4% in the cases where only air and air + Hg were injected into the reactor, respectively. In the case of AC–Br sorbents, a decrease in the mole percentage of Br is only detected when the temperature of the reactor is 140 °C. These results indicate that physisorbed HBr might be desorbing from the surface due to the heat

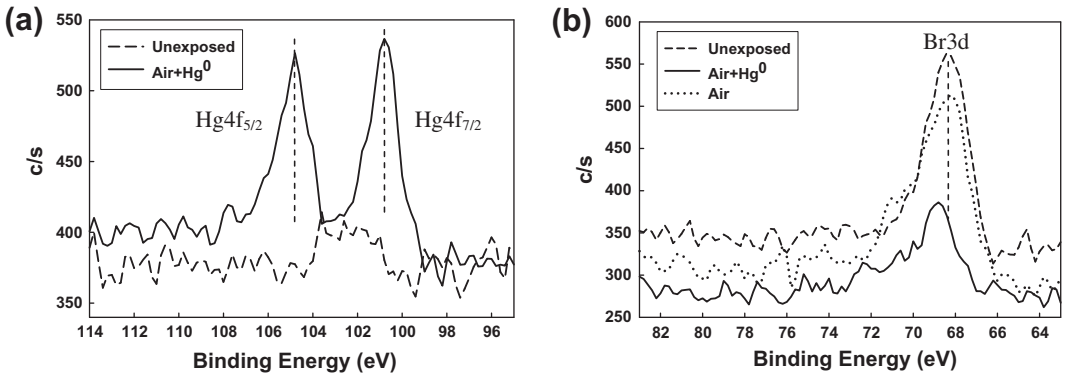

Fig. 3. (a) Hg4f and (b) Br3d core-level XPS spectra for brominated fiber AC sorbent exposed to 403 μg/m^3 Hg^0 at 140 °C.

treatment in the reactor. It is important to note that XPS is a surface-sensitive technique and that these levels of Br detected comprise the Br available at the surface for interacting with Hg^0. As seen in Fig. 3b, the Br3d peak shifts to a higher binding energy after exposure of the ACF–Br sorbent to Hg^0, which indicates that the chemical state of Br has changed. This behavior has also been reported by Qu et al. [36], where they investigate the sorption of Hg on amorphous carbon particles impregnated with halides. The shift was not detected when only air was injected into the reactor, indicating that the chemical state change likely arises from bromine's interactions with Hg^0, possibly to form Hg–Br compounds on the surface. It is important to note that the Br concentration is so much higher than Hg, that there is not sufficient resolution to discern changes to the Br due to interactions with Hg.

The results of the Hg L_{III}-edge EXAFS analysis of the two samples tested in the presence of air and Hg^0 are shown in Fig. 4. The fits are overlaid with the EXAFS spectra and the Fourier Transform of each sample. The resulting parameters used in the EXAFS fitting are reported in Table 3, along with literature values for the bond distances of Hg in the gas phase [37]. As shown in Table 3, the bond distances between Hg and its nearest neighbor are found to be 2.55 ± 0.01 and 2.58 ± 0.01 Å in the case of the AC–Br and ACF–Br sorbents, respectively. This bond distance is significantly larger than that of gas phase Hg–O (2.05 Å), but close to values for gas-phase Hg_2Br_2 (2.62 Å) and $HgBr_2$ (2.41 Å). Fitting of the EXAFS spectra for AC–Br and ACF–Br showed no evidence for either a Hg–O bond or Hg having an oxygen in a second shell coordination (2.1–3.0 Å). Due to C being a weak backscatterer, detecting a Hg–C coordination is often difficult. This difficulty increases with the presence of a strong backscatterer, such as Br, being present in the sample.

In comparison to the Hg^{2+} reference compound (edge of $HgCl_2$ set at 12,284 eV), the main absorption edge inflection points of the Hg/AC–Br and Hg/ACF–Br sorbents are shifted to higher energy values (12,287 eV), indicating the formation of Hg^{2+} compounds (or sorption complexes) rather than Hg^+ compounds in the carbon matrix. In all of the EXAFS spectra, the Hg L_{III} -edge spectra can only be fitted with high accuracy when the coordination number of Hg is 2.4 and 2.38 with respect to Br for the AC–Br 140 °C and ACF–Br 140 °C samples, respectively. These results indicate that Hg^{2+} is bonded to two Br atoms at a distance of 2.55 and 2.58 ± 0.01 Å. The data show no evidence for the presence of Hg^0 within the samples. The possible interaction of Hg with O or another Hg atom was investigated in the EXAFS spectra. A variety of Hg–O single-scattering pathways ranging from 2.1–3.0 Å were created and used during fitting the EXAFS spectra to determine if any Hg–O backscattering pathways existed. All FEFF-generated Hg–O pathways created resulted in the theoretical pathways being complete inverses of the data in a k range of 3–5.25 Å^{-1}. Beyond k = 5.25 Å^{-1} the FEFF-generated

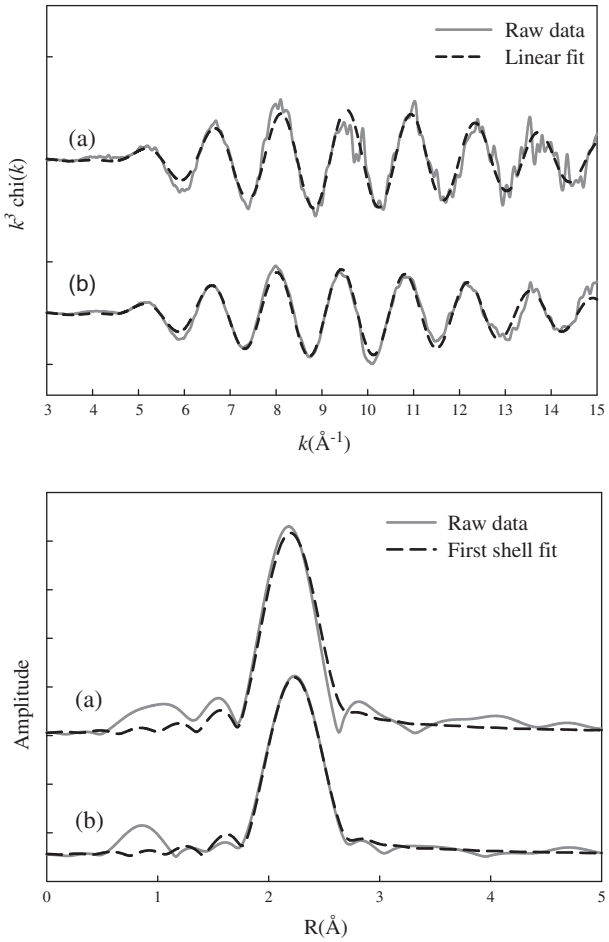

Fig. 4. Fitting results for the AC samples showing the EXAFS spectrum of the samples (gray solid line) and the best linear combination fit (black dash line): (a) AC–Br 403 μg/m^3 140 °C, (b) ACF–Br 403 μg/m^3 140 °C.

pathways were out of phase when compared to the data out to a k = 15 Å^{-1}. Because all of the FEFF-generated Hg–O pathways created from 2.2–3.0 Å were out of phase when compared to the AC samples, a coordination between Hg and O at a distance <3.0 Å is highly unlikely. Though the Hg is considered to be bonded to carbon, it was not detected due to reasons described above. XPS analysis reveals that the surface concentration of O is much higher than that of Br. However, its availability to bind Hg is questionable since the formation of HgO compounds were not detected in the case of non-halogenated AC exposed to Hg^0 and air [9]. It is possible that the

Table 3
Structural parameters of shell-by-shell fitting of the EXAFS spectrum.

	R (Å)	N	ΔE_0	σ^2	Reduced (χ^2)
AC–Br 403 μg/m^3 140 °C	2.55 ± 0.01	2.40 ± 0.13	−1.79 ± 0.87	0.0046 ± 0.0002	13.22
ACF–Br 403 μg/m^3 140 °C	2.58 ± 0.01	2.38 ± 0.07	−0.07 ± 0.44	0.0051 ± 0.0002	33.24
Hg_2Br_2 (g)	2.62				
$HgBr_2$ (g)	2.41				
HgO(g)	2.05				

R: Atomic distance, N: Coordination number, ΔE_0: Energy shift from the theoretical value, σ^2: Debye–Waller factor. The amplitude reduction value is fixed at 0.9 for all the three fits.

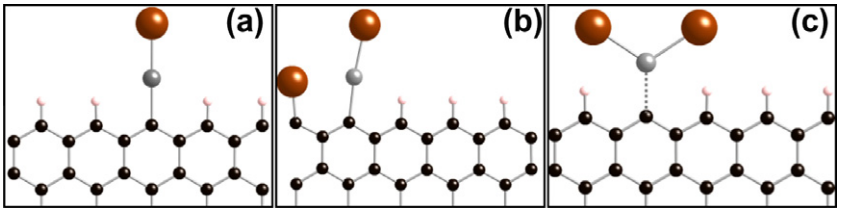

Fig. 5. The optimized graphene structures showing the HgBr and $HgBr_2$ formation on the edge sites of (a) H–H–Hg(Br)–H–H, (b) Br–Hg(Br)–H–H–H and (c) H–Hg(Br_2)–H–H–H. (Atoms are represented as C, black; Br, orange; Hg, gray; H, pink).

Table 4
Energies and bond distances of tested edge-site configurations.

		Distance between atoms[a]				
Structure	Energy (eV)	Br–C_A[b] (Å)	Hg–C_A (Å)	O–C_A (Å)	Br–Hg (Å)	O–Hg (Å)
H–H–Hg(Br)–H–H	−950.724	–	2.10	–	2.45	–
H–H–Br(Hg)–H–H	−950.381	1.91	–	–	3.47	–
H–Br–Hg–H–H	−938.066	1.91	2.35	–	3.01	–
H–Br–H–Hg–H	−938.451	1.91	2.33	–	–	–
Br–Hg–Br–H–H	−932.51	1.94	2.2	–	2.8	–
Br–Hg–H–Br–H	−933.643	1.91	2.33	–	3.03	–
Br–Br(Hg)–H–H–H	−944.493	1.92	–	–	3.73	–
Br–Hg(Br)–H–H–H	−945.92	–	2.08	–	2.45/2.92	–
H–Br–H–Hg(Br)–H	−946.319	1.904	2.095	–	2.444	–
H–Hg(Br_2)–H–H–H	−953.743	–	2.20	–	2.58/2.58	–

[a] Bond distance is given for the two nearest neighbors of given types.
[b] C_A = Surface carbon atom directly below given surface atom.

surface-bound O is not an effective binding site for the adsorption of Hg^0 and does not form a bond with Hg; however, it might assist the surface-bound Br sites to react with Hg^0.

In summary the Hg compound formed on the carbon surface is likely to be $HgBr_2$ at 140 °C. The characterization results of AC and ACF sorbents using both EXAFS spectroscopy and XPS are in good agreement with one other. Our results are also in agreement with the previous studies showing that Hg is oxidized on the carbon surface and the anionic species, e.g. Br, are responsible for Hg capture [5,6].

3.1. Chemical nature of bound mercury species from DFT

Electronic structure calculations based on plane-wave DFT were carried out to determine the surface reactivity and subsequent stability of surface-bound Hg species on simulated AC surfaces, as well as to validate the geometries and adsorption mechanisms postulated from the XPS and EXAFS analysis. The investigated structures are represented with surfaces that contain five edge sites (on each side of the graphene ribbon). Each structure is labeled in the form "X–X–X–X–X" where the five letters represent the surface coverage of five zigzag edge sites of the graphene they are bound to, as shown in Fig. 5. Additionally, "–X(Y)–" and "–X–(Y)–X–" denote an additional atom Y positioned above the surface atom X, and above and between the two X atoms, respectively. The DFT-calculated surfaces include various combinations of -H, -Br, and -Hg bound at an edge site. The effect of O on the binding of Hg in the presence of Br atoms has also been considered. Oxygen is found to decrease the DFT energy (more stable) of the structure when it is located at the neighboring carbon edge site of the bound Hg atom; however, our previous work indicated that the edge C binds to Hg more tightly when it is located next to a surface O atom, but not immediately next to a bound Br atom [23]. In some combinations, such as the H–H–Hg(Br)–H–H and H–Br–H–Hg(Br)–H structures, the optimized final structures and DOS are found to be similar and the effect of the Br on the binding of Hg is negligible when they are not located at the neighboring graphene edge site Table 4. provides the energy of each of the system configurations tested in addition to the bond length of neighboring atoms. Configurations are grouped in clusters with consistent type and number of atoms, so that DFT energies may be compared directly to determine which configuration results in the more stable surface (edge). The lowest DFT energy in each cluster corresponds to the thermodynamically most stable structure. As shown in Table 4, the binding of Hg to the surface-bound Br is found to be 0.34 eV less stable in the case of the H–H–Br(Hg)–H–H structure in comparison to a

corresponding structure where Br binds to the surface-bound Hg(H–H–Hg(Br)–H–H). As shown in Fig. 5, a linear C–Hg–Br molecule forms on the graphene edge site with Hg–Br and Hg–C bond distances of 2.45 Å and 2.1 Å, respectively. A similar interaction was also observed in a previous study where Padak and Wilcox carried out a Mulliken bond population analysis of Hg and chlorine (Cl) structures bound on four-ring graphene clusters using DFT [22]. They reported that the C–Hg bond was stronger when Hg was bound to the graphene edge site interacting with the Cl atom bound atop of Hg, which is in agreement with the current work. Additionally, a comparison of the DFT energies of the H–Br–Hg–H–H and H–Br–H–Hg–H structures reveals that the Hg–Br interaction can be repulsive when both Hg and Br are bound to neighboring carbon edge sites. The bond distance of Hg–Br is found to be larger in H–Br–Hg–H–H than that obtained in the EXAFS analysis, indicating that this configuration is not likely the structure formed on the surface.

In addition to a single Br interaction, the effect of two Br atoms on Hg binding has been investigated and reported in Table 4. It has been observed that Hg is more stable if it interacts directly with the C edge site, while making additional bonds with Br atoms. In the case of the Br–Br(Hg)–H–H–H structure, the interaction between Hg and surface bound Br is repulsive and the Hg–Br bond distance is found to be 3.73 Å. Again, as with the single Br structures, a surface-bound Br adjacent to a surface bound Hg or Hg(Br) complex is thermodynamically unstable in comparison to a corresponding structure where the Br and Hg are separated by a surface-bound H. For instance, the DFT energy of H–Br–H–Hg(Br)–H is 0.4 eV lower than that of Br–Hg(Br)–H–H–H. In the case of the Br–Hg(Br)–H–H–H structure, the vertical and adjacent Hg–Br bond distances are found to be 2.45 Å and 2.95 Å, respectively and do not match the EXAFS results. The bond distance predicted between Hg and the surface-bound Br atom is large in comparison to those found in the gas phase and on the graphene edge site. An additional calculation, i.e. the H–Hg(Br_2)–H–H–H structure, was carried out with two Br atoms and reveals a Hg–Br bond distance is 2.58 Å. The hydrogen atoms bound to graphene edge sites decrease the effect of the C–Br interaction leading to a smaller Hg–Br bond distance in comparison to the Br–Hg–Br–H–H structure. The Hg–Br bond distance in the H–Hg(Br_2)–H–H–H structure matches well with the EXAFS analysis, and the stability of the $HgBr_2$-type structures will be discussed in the following DOS analysis.

3.2. Density of states (DOS) analysis

To further investigate Hg–Br and Hg-surface C (C_A) interactions, a DOS analysis was undertaken for the Hg–Br–H–H–H, H–H–Hg(Br)–H–H, Br–Hg(Br)–H–H–H, and H–Hg(Br_2)–H–H–H structures. Comparing the DOS of similar systems, one can determine the relative strength of the bond of particular atoms. Fig. 6 shows DOS results for s- and p- states of C_A and Br; and s-, p- and d- states of Hg adsorbed in the (a) H–H–Hg(Br)–H–H, (b) Br–Hg(Br)–H–H–H, and (c) H–Hg(Br_2)–H–H–H structures. A comparison of the Hg DOS pre-adsorption (gas phase, not shown) and post-adsorption (on the surface) shows that Hg p-states play the most significant role in the adsorption process. While gas-phase Hg s-, p- and d- states show single peaks at −1 eV, 4.8 eV and −4 eV, respectively, they shift to more negative energy values and split into multiple peaks upon adsorption. The hybridization of Hg s- and Hg p-states with the Br p-state is clearly seen in the four structures shown in Fig. 6. However, an interaction between the Hg p-states and Br p-states is not observed in the case of the H–Br–Hg–H–H structure (not shown), indicating a weaker Hg bonding. Furthermore, in this structure the Hg s- and p-states located at the Fermi level are partly occupied and only interacting with C p-states. In the case of the H–H–Hg(Br)–H–H structure, the Hg s-, p- and d- bonding states are

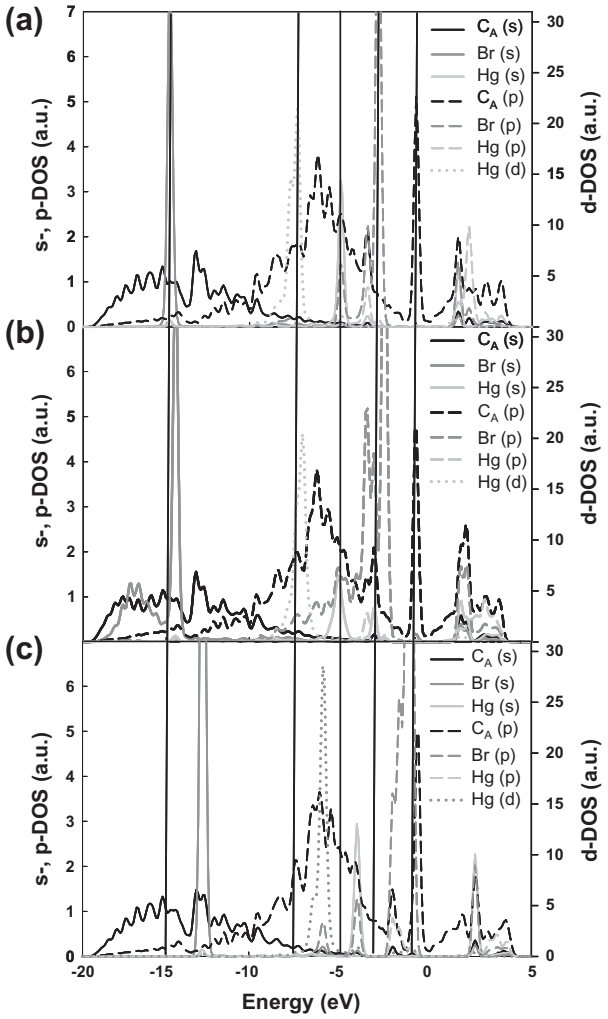

Fig. 6. DOS comparing adsorbed Hg on (a) H–H–Hg(Br)–H–H, (b) Br–Hg(Br)–H–H–H and (c) H–Hg(Br_2)–H–H–H structures.

shifted below the Fermi level and are located at more negative energies than that of the other three structures. This observation indicates that, for the configurations investigated, the C–Hg bond is strongest when HgBr is bound to the edge C atom with the Hg. When Br is attached to the edge site of graphene, i.e. in the H–Br–Hg–H–H (not shown) and Br–Hg(Br)–H–H–H–H structures, the Br s-states interact with the C_A s-states at approximately −17 eV. In addition, the Br p-states interact with the Hg d- and C_A p-states at −6 eV. These interactions are not observed in the case of the H–H–Hg(Br)–H–H structure, where Br is only located at the top of Hg without attaching to the edge site of graphene. In all the structures investigated the C_A s-states do not show significant change, where as the first moment of the C_A p-bonding states shift down due to the interaction between Hg and Br in the case of the H–H–Hg(Br)–H–H structure. When Br s- and p-states are compared in Fig. 6, they are found to be closest to the Fermi energy in the case of the H–Hg(Br_2)–H–H–H structure, indicating that the Hg–Br bonds of Hg(Br_2) are less stable, although the Hg–Br bond distance is found to match well with the EXAFS analysis.

EXAFS characterization indicates that Hg is oxidized in the carbon surface pores and forms Hg^{2+} compounds interacting with two Br atoms. Additionally, EXAFS analysis reveals that neither O nor a second Hg was located adjacent to Hg in the samples characterized. The optimized structures reported in this study show that Hg is most stable bound directly to a surface carbon. Mercury interaction

with brominated AC likely involves Hg interaction with the surface-bound Br by possibly detaching/replacing it from the graphene edge site. The effect of O on the binding of Hg in the presence of Br atom has been investigated in our previous work [10]. It was found that the edge C binds to Hg more tightly when it is located next to a surface O atom, but not immediately next to a bound Br atom [10]. It is possible that Hg surface reactions on the carbon surface are kinetically controlled, as observed in Hg gas phase reactions [38], and that the most stable structures found on DFT simulations may not form on the carbon surface. Given the results, we think that although Hg(Br) and Hg–O species investigated in the current and previous [10] works are more stable on the surface, the activation barriers of surface intermediate reactions may lead to the stable formation of Br–Hg(Br) and $Hg(Br_2)$ type species on graphene edge sites. The bond distances of Br–Hg(Br) and $Hg(Br_2)$ type structures are found to be closer to our EXAFS analysis results, and it is possible that surface-bound Br may not form an actual bond with Hg. Since Br–Hg(Br) and $Hg(Br_2)$ type species are not strongly bound on the graphene edge site, they may desorb from the surface when a more acidic species (i.e. SO_2) is present.

4. Conclusion

The speciation of Hg adsorbed on brominated AC sorbents has been investigated in the presence of air. Both XPS and EXAFS experimental characterization results reveal that Hg is adsorbed on brominated AC as Hg^{2+} at both 30 °C and 140 °C, indicating that chemisorption is the likely adsorption mechanism of Hg. Fitting of the EXAFS spectra shows that Hg interacts with two Br atoms at a distance of 2.55 and 2.58 ± 0.01 Å inside the C matrix. Plane-wave DFT calculations reveal that Hg s- and Hg p-states hybridize with Br and C p-states to form stable complexes on graphene edge sites. The interaction between C and Hg is possibly strong enough to detach Br from the graphene edge site, so that Hg can bind to the surface C directly. Although the C–Hg bond is more stable when Hg only interacts with one Br atom bound atop of Hg, relatively less stable complexes, i.e. Hg(Br)Br and $Hg(Br_2)$, can also form on the surface. Additional surface characterization experiments of AC sorbents will be carried out in the future using both XPS and EXAFS spectroscopy to identify the role of other flue gas species and halogens on Hg adsorption and its subsequent oxidation.

Acknowledgments

The authors acknowledge the financial support provided by Electric Power Research Institute (EPRI), along with valuable discussions with Ramsay Chang. The computations were carried out on the Center for Computational Earth & Environmental Science (CEES) cluster at Stanford University. We wish to thank Matthew Latimer of the Stanford Synchrotron Radiation Lightsource for his assistance with data collection on beamline 7-3. D.A.B. gratefully acknowledges support by the Stanford Graduate Fellowship program. Portions of this research were carried out at the Stanford Synchrotron Radiation Lightsource, a National user facility operated by Stanford University on behalf of the US Department of Energy, Office of Basic Energy Science, with additional support from the National Institute of Health. We wish to thank Chuck Hitzman in operating the PHI VersaProbe Scanning XPS Microprobe at the Stanford Nanocharacterization Laboratory.

References

[1] US environmental protection agency. Clean air mercury rule. <http://www.epa.gov/airquality/powerplanttoxics/>; 2011 [retrieved on 23.04.2011].
[2] Pirrone N, Cinnirella S, Feng X, et al. Global mercury emissions to the atmosphere from anthropogenic and natural sources. Atmos Chem Phys Discuss 2010;10:4719–52.
[3] Hower JC, Senior CL, Suuburg EM, Hurt RH, Wilcox J, Olson ES. Mercury capture by native fly ash carbons in coal-fired power plants. Prog Energy Combust Sci 2010;36:510–29.
[4] Chen S, Rostam-Abadi M, Chang R. Mercury removal from combustion flue gas by activated carbon injection: mass transfer. Pap – Am Chem Soc, Div Fuel Chem 1996;41:442–6.
[5] Huggins FE, Yap N, Huffman GP, Senior CL. XAFS characterization of mercury captured from combustion gases on sorbents at low temperatures. Fuel Process Technol 2003;82(2–3):167–96.
[6] Hutson ND, Attwood BC, Scheckel KG. XAS and XPS characterization of mercury binding on brominated activated carbon. Environ Sci Technol 2007;41(5):1747–52.
[7] Olson ES, Azenkeng A, Laumb JD, Jensen RR, Benson SA, Hoffman MR. New developments in the theory and modeling of mercury oxidation and binding on activated carbons in flue gas. Fuel Process Technol 2009;90:1360–3.
[8] Laumb JD, Benson SA, Olson ES. X-ray photoelectron spectroscopy analysis of mercury sorbent surface chemistry. Fuel Process Technol 2004;85:577–85.
[9] Rostam-Abadi M, Lu Y, Chang R, Shaban C, Botha F. Production of activated carbon for mercury emission control: bench-scale testing of a sorbent activation process unit. In: Proceedings of air & waste manage assoc MI, USA: Detroit; 2009.
[10] Wilcox J, Sasmaz E, Kirchofer A, Lee S-S. Heterogeneous mercury reaction chemistry on activated carbon. J Air Waste Manage Assoc 2011;61:418–26.
[11] PHI multipak softwareTM. Japan: Ulvac-phi Inc.; 2006.
[12] Jew AD, Kim CS, Rytuba JJ, Gustin MS, Brown GE. New technique for quantification of elemental hg in mine wastes and its implications for mercury evasion into the atmosphere. Environ Sci Technol 2011;45:412–8.
[13] Ankudinov AL, Ravel B, Rehr JJ, Conradson SD. Real-space multiple-scattering calculation and interpretation of X-ray-absorption near-edge structure. Phys Rev B 1998;58(12):7565–76.
[14] Webb S. SixPACK version 0.67. stanford synchrotron radiation lightsource. Menlo Park, CA, USA; 2006.
[15] Webb SM. A graphical user interface for XAS analysis using. IFEFFIT Phys Scr 2005;T115:1011–4.
[16] Kresse G, Hafner J. Ab-initio molecular dynamics for liquid metals. Phys Rev B 1993;48:13115–7;
Kresse G, Furthmuller J. Efficiency of ab-initio total energy calculations for metals and semiconductors using a plane-wave basis set. Comput Mater Sci 1996;6:15–50.
[17] Blöchl PE. Projector augmented-wave method. Phys Rev B 1994;50:17953–79; Kresse G, Joubert D. From ultrasoft pseudopotentials to the projector augmented-wave method. Phys Rev B 1999;59:1758–75.
[18] Perdew JP, Burke K, Ernzerhof M. Generalized gradient approximation made simple. Phys Rev Lett 1996;77:3865–8.
[19] Methfessel M, Paxton AT. High-precision sampling for Brillouin-zone integration in metals. Phys Rev B 1989;40:3616–21.
[20] Monkhorst HJ, Pack JD. Special points for Brillouin-zone integrations. Phys Rev B 1976;13:5188–92.
[21] Radovic LR. The mechanism of CO_2 chemisorption on zigzag carbon active sites: a computational chemistry study. Carbon 2005;43:907–15.
[22] Padak B, Wilcox J. Understanding mercury binding on activated carbon. Carbon 2009;47(12):2855–64.
[23] Radovic LR, Bockrath B. On the chemical nature of graphene edges: origin of stability and potential for magnetism in carbon materials. J Am Chem Soc 2005;127:5917–27.
[24] Yang FH, Yang RT. Ab initio molecular orbital study of adsorption of atomic hydrogen on graphite: Insight into hydrogen storage in carbon nanotubes. Carbon 2002;40:437–44.
[25] Menendez JA, Xia B, Phillips J, Radovic LR. On the modification and characterization of chemical surface properties of activated carbon: microcalorimetric, electrochemical, and thermal desorption probes. Langmuir 1997;13:3414–21.
[26] Montoya A, Truong TN, Sarofim AF. Spin contamination in hartree-fock and density functional theory wavefunctions in modeling of adsorption on graphite. J Phys Chem A 2000;104:8409–17.
[27] Presto A, Granite EJ. Impact of sulfur oxides on mercury capture by activated carbon. Environ Sci Technol 2007;41:6579–84.
[28] Olson ES, Crocker CR, Benson SA, Pavlish JH, Holmes MJ. Surface compositions of carbon sorbents exposed to simulated low-rank coal flue gases. J Air Waste Manage Assoc 2005;55:747–54.
[29] Briggs D, Seah MP. Practical surface analysis. Appendix 5. New York: John Wiley & Sons Inc.; 1996.
[30] NIST X-ray photoelectron spectroscopy database. NIST standard reference database 20. Version 3.5. <http://srdata.nist.gov/xps/Default.aspx>; 2008 [retrieved on 15.06.08].
[31] Vidic RD, Siler DP. Vapor-phase elemental mercury adsorption by activated carbon impregnated with chloride and chelating agents. Carbon 2001;39:3.
[32] Basu R, Kinser CR, Tovar JD, Hersam MC. Bromine functionalized molecular adlayers on hydrogen passivated silicon surfaces. Chem Phys 2006;326:144–50.
[33] Papirer E, Lacroix R, Donnett JB, Nanse G, Fioux P. XPS study of the halogenation of carbon black – Part 1. Bromination. Carbon 1994;32:1341–58.

[34] Duesberg GS, Roth S, Downes P, Minett A, Graupner R, Lothar L, et al. Modification of single-walled carbon nanotubes by hydrothermal treatment. Chem Mater 2003;15:3314.
[35] Budarin VL, Clark JH, Tavener SJ, Wilson K. Chemical reactions of double bonds in activated carbon: microwave and bromination methods. Chem Commun 2004;23:2736–7.
[36] Qu Z, Chang JJ, Hsiung T, et al. Halides on carbonaceous materials for enhanced capture of Hg^0: mechanistic study. Energy Fuels 2010;24:3534–9.
[37] Tossell JA. Calculation of the energetics for oxidation of gas-phase elemental Hg by Br and BrO. J Phys Chem A 2003;107:7804–8.
[38] Senior CL, Sarofim AL, Zeng T, Helble JJ, Mamani-Paco R. Gas-phase transformations of mercury in coal-fired power plants. Fuel Process Technol 2000;63:197.